
Conservative State Value Estimation for Offline Reinforcement Learning

Liting Chen*
McGill University
Montreal, Canada
98chenliting@gmail.com

Jie Yan †
Microsoft
Beijing, China
dasistyanjie@gmail.com

Zhengdao Shao*
University of Sci. and Tech. of China
Hefei, China
zhengdaoshao@mail.ustc.edu.cn

Lu Wang
Microsoft
Beijing, China
wlu@microsoft.com

Qingwei Lin
Microsoft
Beijing, China
qlin@microsoft.com

Saravan Rajmohan
Microsoft 365
Seattle, USA
saravar@microsoft.com

Thomas Moscibroda
Microsoft
Redmond, USA
moscitho@microsoft.com

Dongmei Zhang
Microsoft
Beijing, China
dongmeiz@microsoft.com

Abstract

Offline reinforcement learning faces a significant challenge of value over-estimation due to the distributional drift between the dataset and the current learned policy, leading to learning failure in practice. The common approach is to incorporate a penalty term to reward or value estimation in the Bellman iterations. Meanwhile, to avoid extrapolation on out-of-distribution (OOD) states and actions, existing methods focus on conservative Q-function estimation. In this paper, we propose Conservative State Value Estimation (CSVE), a new approach that learns conservative V-function via directly imposing penalty on OOD states. Compared to prior work, CSVE allows more effective state value estimation with conservative guarantees and further better policy optimization. Further, we apply CSVE and develop a practical actor-critic algorithm in which the critic does the conservative value estimation by additionally sampling and penalizing the states *around* the dataset, and the actor applies advantage weighted updates extended with state exploration to improve the policy. We evaluate in classic continual control tasks of D4RL, showing that our method performs better than the conservative Q-function learning methods and is strongly competitive among recent SOTA methods.

1 Introduction

Reinforcement Learning (RL) learns to act by interacting with the environment and has shown great success in various tasks. However, in many real-world situations, it is impossible to learn from scratch online as exploration is often risky and unsafe. Instead, offline RL ([1, 2]) avoids this problem by learning the policy solely from historical data. Yet, simply applying standard online RL techniques to static datasets can lead to overestimated values and incorrect policy decisions when faced with unfamiliar or out-of-distribution (OOD) scenarios.

*Work done during the internship at Microsoft. † Work done during full-time employment at Microsoft.

Recently, the principle of conservative value estimation has been introduced to tackle challenges in offline RL[3, 4, 5]. Prior methods, e.g., CQL(Conservative Q-Learning [4]), avoid the value over-estimation problem by systematically underestimating the Q values of OOD actions on the states in the dataset. In practice, it is often too pessimistic and thus leads to overly conservative algorithms. COMBO [6] leverages a learned dynamic model to augment data in an interpolation way. This process helps derive a Q function that’s less conservative than CQL, potentially leading to more optimal policies.

In this paper, we propose CSVE (Conservative State Value Estimation), a novel offline RL approach. Unlike the above methods that estimate conservative values by penalizing the Q-function for OOD actions, CSVE directly penalizes the V-function for OOD states. We theoretically demonstrate that CSVE provides tighter bounds on in-distribution state values in expectation than CQL, and same bounds as COMBO but under more general discounted state distributions, which potentially enhances policy optimization in the data support. Our main contributions include:

- The conservative state value estimation with related theoretical analysis. We prove that it lower bounds the real state values in expectation over any state distribution that is used to sample OOD states and is up-bounded by the real state values in expectation over the marginal state distribution of the dataset plus a constant term depending on sampling errors. Compared to prior work, it enhances policy optimization with conservative value guarantees.
- A practical actor-critic algorithm implemented CSVE. The critic undertakes conservative state value estimation, while the actor uses advantage-weighted regression(AWR) and explores states with conservative value guarantee to improve policy. In particular, we use a dynamics model to sample OOD states that are directly reachable from the dataset, for efficient value penalizing and policy exploring.
- Experimental evaluation on continuous control tasks of Gym [7] and Adroit [8] in D4RL [9] benchmarks, showing that CSVE performs better than prior methods based on conservative Q-value estimation, and is strongly competitive among main SOTA algorithms.

2 Preliminaries

Offline Reinforcement Learning. Consider the Markov Decision Process $M := (\mathcal{S}, \mathcal{A}, P, r, \rho, \gamma)$, which comprises the state space \mathcal{S} , the action space \mathcal{A} , the transition model $P : \mathcal{S} \times \mathcal{A} \rightarrow \Delta(\mathcal{S})$, the reward function $r : \mathcal{S} \times \mathcal{A} \rightarrow \mathbb{R}$, the initial state distribution ρ and the discount factor $\gamma \in (0, 1]$. A stochastic policy $\pi : \mathcal{S} \rightarrow \mathcal{A}$ selects an action probabilistically based on the current state. A transition is the tuple (s_t, a_t, r_t, s_{t+1}) where $a_t \sim \pi(\cdot|s_t)$, $s_{t+1} \sim P(\cdot|s_t, a_t)$, and $r_t = r(s_t, a_t)$. It’s assumed that the reward values adhere to $|r(s, a)| \leq R_{max}, \forall s, a$. A trajectory under π is the random sequence $\tau = (s_0, a_0, r_0, s_1, a_1, r_1, \dots, s_T)$ which consists of continuous transitions starting from $s_0 \sim \rho$.

Standard RL is to learn a policy $\pi \in \Pi$ that maximize the expected cumulative future rewards, represented as $J_\pi(M) = \mathbb{E}_{M, \pi}[\sum_{t=0}^{\infty} \gamma^t r_t]$, through active interaction with the environment M . At any time t , for the policy π , the value function of state is defined as $V^\pi(s) := \mathbb{E}_{M, \pi}[\sum_{k=0}^{\infty} \gamma^{t+k} r_{t+k} | s_t = s]$, and the Q value function is $Q^\pi(s, a) := \mathbb{E}_{M, \pi}[\sum_{k=0}^{\infty} \gamma^{t+k} r_{t+k} | s_t = s, a_t = a]$. The Bellman operator is a function projection: $\mathcal{B}^\pi Q(s, a) := r(s, a) + \gamma \mathbb{E}_{s' \sim P(\cdot|s, a), a' \sim \pi(\cdot|s')} [Q(s', a')]$, or $\mathcal{B}^\pi V(s) := \mathbb{E}_{a \sim \pi(\cdot|s)} [r(s, a) + \gamma \mathbb{E}_{s' \sim P(\cdot|s, a)} [V(s')]]$, resulting iterative value updates. Bellman consistency implies that $V^\pi(s) = \mathcal{B}^\pi V^\pi(s), \forall s$ and $Q^\pi(s) = \mathcal{B}^\pi Q^\pi(s, a), \forall s, a$. When employing function approximation in practice, the empirical Bellman operator $\hat{\mathcal{B}}^\pi$ is used, wherein the aforementioned expectations are estimated with data. Offline RL aims to learn the policy π from a static dataset $D = \{(s, a, r, s')\}$ made up of transitions collected by any behavior policy, with the objective of performing well in the online setting. Note that, unlike standard online RL, offline RL does not interact with the environment during the learning process.

Conservative Value Estimation. One main challenge in offline RL arises from the over-estimation of values due to extrapolation in unseen states and actions. Such overestimation can lead to the deterioration of the learned policy. To address this issue, conservatism or pessimism is employed in value estimation. For instance, CQL learns a conservative Q-value function by penalizing the value

of unseen actions:

$$\hat{Q}^{k+1} \leftarrow \arg \min_Q \frac{1}{2} \mathbb{E}_{s,a,s' \sim D} [(Q(s,a) - \hat{\beta}_\pi \hat{Q}^k(s,a))^2] + \alpha (\mathbb{E}_{\substack{s \sim D \\ a \sim \mu(\cdot|s)}} [Q(s,a)] - \mathbb{E}_{\substack{s \sim D \\ a \sim \hat{\pi}_\beta(\cdot|s)}} [Q(s,a)]) \quad (1)$$

where $\hat{\pi}_\beta$ and π are the behaviour policy and learnt policy separately, μ is an arbitrary policy different from $\hat{\pi}_\beta$, and α represents the factor for balancing conservatism.

Constrained Policy Optimization. To address the issues of distribution shift between the learning policy and the behavior policy, one approach is to constrain the learning policy close to the behavior policy [10, 11, 12, 13, 1]. As an example, AdvantageWeighted Regression(AWR)[14, 12] employs an implicit KL divergence to regulate the distance between policies:

$$\pi^{k+1} \leftarrow \arg \max_\pi \mathbb{E}_{s,a \sim D} \left[\frac{\log \pi(a|s)}{Z(s)} \exp \left(\frac{1}{\lambda} A^{\pi^k}(s,a) \right) \right]$$

Here, A^{π^k} is the advantage of policy π^k , and Z serves as the normalization constant for s .

Model-based Offline RL. In RL, the model is an approximation of the MDP M . Such a model is denoted as $\hat{M} := (\mathcal{S}, \mathcal{A}, \hat{P}, \hat{r}, \rho, \gamma)$, with \hat{P} and \hat{r} being approximation of P and r respectively. Within offline RL, the model is commonly used to augment data [15, 6] or act as a surrogate of the real environment during interaction [16]. However, such practices can inadvertently introduce bootstrapped errors over extended horizons[17]. In this paper, we restrict the use of the model to one-step sampling on the next states that are approximately reachable from the dataset.

3 Conservative State Value Estimation

In the offline setting, the value overestimation is a major problem resulting in failure of learning a reasonable policy [13, 1]. In contrast to prior works[4, 6] that get conservative value estimation via penalizing Q function for OOD state-action pairs, we directly penalize V function for OOD states. Our approach provides several novel theoretic results that allow better trade-off of conservative value estimation and policy improvement. All proofs of our theorems can be found in Appendix A.

3.1 Conservative Off-policy Evaluation

We aim to conservatively estimate the value of a target policy using a dataset to avoid overestimation of OOD states. To achieve this, we penalize V-values evaluated on states that are more likely to be OOD and increase the V-values on states that are in the distribution of the dataset. This adjustment is made iteratively::

$$\hat{V}^{k+1} \leftarrow \arg \min_V \frac{1}{2} \mathbb{E}_{s \sim d_u(s)} [(\hat{\mathcal{B}}^\pi \hat{V}^k(s) - V(s))^2] + \alpha (\mathbb{E}_{s' \sim d(s)} V(s') - \mathbb{E}_{s \sim d_u(s)} V(s)) \quad (2)$$

where $d_u(s)$ is the discounted state distribution of D , $d(s)$ is any state distribution, and $\hat{\mathcal{B}}^\pi$ is the empirical Bellman operator (see appendix for more details). Considering the setting without function approximation, by setting the derivative of Eq. 2 as zero, we can derive the V function using approximate dynamic programming at iteration k ::

$$\hat{V}^{k+1}(s) = \hat{\mathcal{B}}^\pi \hat{V}^k(s) - \alpha \left[\frac{d(s)}{d_u(s)} - 1 \right], \quad \forall s, k. \quad (3)$$

Denote the function projection on \hat{V}^k in Eq. 3 as \mathcal{T}^π . We have Lemma 3.1, which ensures that \hat{V}^k converges to a unique fixed point.

Lemma 3.1. For any d with $\text{supp } d \subseteq \text{supp } d_u$, \mathcal{T}^π is a γ -contraction in L_∞ norm.

Theorem 3.2. For any d with $\text{supp } d \subseteq \text{supp } d_u$ ($d \neq d_u$), with a sufficiently large α (i.e., $\alpha \geq \frac{C_{r,t,\delta} R_{max}}{(1-\gamma)\sqrt{|D(s,a)|}} / \mathbb{E}_{s \sim d(s)} \left[\frac{d(s)}{d_u(s)} - 1 \right]$), the expected value of the estimation $\hat{V}^\pi(s)$ under $d(s)$ is the lower bound of the true value, that is: $\mathbb{E}_{s \sim d(s)} [\hat{V}^\pi(s)] \leq \mathbb{E}_{s \sim d(s)} [V^\pi(s)]$.

$\hat{V}^\pi(s) = \lim_{k \rightarrow \infty} \hat{V}^k(s)$ is the converged value estimation with the dataset D , and $\frac{C_{r,t,\delta} R_{max}}{(1-\gamma)\sqrt{|D(s,a)|}}$ is related to sampling error that arises when using the empirical operator instead of the Bellman operator. If the counts of each state-action pair is greater than zero, $|D(s,a)|$ denotes a vector of size $|\mathcal{S}||\mathcal{A}|$ containing counts for each state-action pair. If the counts of this state action pair is zero, the corresponding $\frac{1}{\sqrt{|D(s,a)|}}$ is a large yet finite value. We assume that with probability $\geq 1 - \delta$, the sampling error is less than $\frac{C_{r,t,\delta} R_{max}}{(1-\gamma)\sqrt{|D(s,a)|}}$, while $C_{r,t,\delta}$ is a constant (See appendix for more details.) Note that if the sampling error can be disregarded, $\alpha > 0$ can ensure the lower bound results.

Theorem 3.3. *The expected value of the estimation, $\hat{V}^\pi(s)$, under the state distribution of the original dataset is the lower bound of the true value plus the term of irreducible sampling error. Formally:*

$$\mathbb{E}_{s \sim d_u(s)}[\hat{V}^\pi(s)] \leq \mathbb{E}_{s \sim d_u(s)}[V^\pi(s)] + \mathbb{E}_{s \sim d_u(s)}(I - \gamma P^\pi)^{-1} \mathbb{E}_{a \sim \pi(a|s)} \frac{C_{r,t,\delta} R_{max}}{(1-\gamma)\sqrt{|D(s,a)|}}$$

where P^π refers to the transition matrix coupled with policy π (see Appendix for details).

Now we show that, during iterations, the gap between the estimated V-function values of in-distribution states and OOD states is higher compared to the true V-functions.

Theorem 3.4. *For any iteration k , given a sufficiently large α , our method amplifies the difference in expected V-values between the selected state distribution and the dataset state distribution. This can be represented as:* $\mathbb{E}_{s \sim d_u(s)}[\hat{V}^k(s)] - \mathbb{E}_{s \sim d(s)}[\hat{V}^k(s)] > \mathbb{E}_{s \sim d_u(s)}[V^k(s)] - \mathbb{E}_{s \sim d(s)}[V^k(s)]$.

Our approach, which penalizes the V-function for OOD states, promotes a more conservative estimate of a target policy’s value in offline reinforcement learning. Consequently, our policy extraction ensures actions align with the dataset’s distribution.

To apply our approach effectively in offline RL algorithms, the preceding theorems serve as guiding principles. Here are four key insights for practical use of Eq. 2:

Remark 1. According to Eq. 2, if $d = d_u$, the penalty for OOD states diminishes. This means that the policy will likely avoid states with limited data support, preventing it from exploring unseen actions in such states. While AWAC [12] employs this configuration, our findings indicate that by selecting a d , our method surpasses AWAC’s performance.

Remark 2. Theorem 3.3 suggests that under d_u , the marginal state distribution of data, the expectation estimated value of V^π is either lower than its true value or exceed it, but within a certain limit. This understanding drives our adoption of the advantage-weighted policy update, as illustrated in Eq. 9.

Remark 3. As per Theorem 3.2, the expected estimated value of a policy under d , which represents the discounted state distribution of any policy, must be a lower bound of its true value. Grounded in this theorem, our policy enhancement strategy merges an advantage-weighted update with an additional exploration bonus, showcased in Eq. 10.

Remark 4. Theorem 3.4 states $\mathbb{E}_{s \sim d(s)}[V^k(s)] - \mathbb{E}_{s \sim d(s)}[\hat{V}^k(s)] > \mathbb{E}_{s \sim d_u(s)}[V^k(s)] - \mathbb{E}_{s \sim d_u(s)}[\hat{V}^k(s)]$. In simpler terms, the underestimation of value is more pronounced under d . With the proper choice of d , we can confidently formulate a newer and potentially superior policy using \hat{V}^k . Our algorithm chooses the distribution of model predictive next-states as d , i.e., $s' \sim d$ is implemented by $s \sim D, a \sim \pi(\cdot|s), s' \sim \hat{P}(\cdot|s, a)$, which effectively builds a soft ‘river’ with low values encircling the dataset.

Comparison with prior work: CQL (Eq.1), which penalizes Q-function of OOD actions, guarantees the lower bounds on state-wise value estimation: $\hat{V}^\pi(s) = E_{\pi(a|s)}(\hat{Q}^\pi(s, a)) \leq E_{\pi(a|s)}(Q^\pi(s, a)) = V^\pi(s)$ for all $s \in D$. COMBO, which penalizes the Q-function for OOD states and actions of interpolation of history data and model-based roll-outs, guarantees the lower bound of state value expectation: $\mathbb{E}_{s \sim \mu_0}[\hat{V}^\pi(s)] \leq \mathbb{E}_{s \sim \mu_0}[V^\pi(s)]$ where μ_0 is the initial state distribution (Remark 1, section A.2 of COMBO [6]); which is a special case of our result in Theorem 3.2 when $d = \mu_0$. Both CSVE and COMBO intend to enhance performance by transitioning from individual state values to expected state values. However, CSVE offers the same lower bounds but under a more general state distribution. Note that μ_0 depends on the environment or the dynamic model during offline training. CSVE’s flexibility, represented by d , ensures conservative guarantees across any discounted state distribution of the learned policy, emphasizing a preference for penalizing V over the Q-function.

3.2 Safe Policy Improvement Guarantees

Now we show that our method has the safe policy improvement guarantees against the data-implied behaviour policy. We first show that our method optimizes a penalized RL empirical objective:

Theorem 3.5. *Let \hat{V}^π be the fixed point of Eq. 3, then $\pi^*(a|s) = \arg \max_\pi \hat{V}^\pi(s)$ is equivalently obtained by solving:*

$$\pi^* \leftarrow \arg \max_\pi J(\pi, \hat{M}) - \frac{\alpha}{1 - \gamma} \mathbb{E}_{s \sim d_M^\pi} \left[\frac{d(s)}{d_u(s)} - 1 \right]. \quad (4)$$

Building upon Theorem 3.5, we show that our method provides a ζ -safe policy improvement over π_β .

Theorem 3.6. *Let $\pi^*(a|s)$ be the policy obtained in Eq. 4. Then, it is a ζ -safe policy improvement over $\hat{\pi}^\beta$ in the actual MDP M , i.e., $J(\pi^*, M) \geq J(\hat{\pi}^\beta, M) - \zeta$ with high probability $1 - \delta$, where ζ is given by:*

$$\begin{aligned} \zeta = & 2 \left(\frac{C_{r,\delta}}{1 - \gamma} + \frac{\gamma R_{max} C_{T,\delta}}{(1 - \gamma)^2} \right) \mathbb{E}_{s \sim d_M^{\pi^*}(s)} \left[c \sqrt{\mathbb{E}_{a \sim \pi(a|s)} \left[\frac{\pi(a|s)}{\pi_\beta(a|s)} \right]} \right] \\ & - \underbrace{(J(\pi^*, \hat{M}) - J(\hat{\pi}^\beta, \hat{M}))}_{\geq \alpha \frac{1}{1 - \gamma} \mathbb{E}_{s \sim d_M^{\pi^*}(s)} \left[\frac{d(s)}{d_u(s)} - 1 \right]} \text{ where } c = \sqrt{|\mathcal{A}|} / \sqrt{|\mathcal{D}(s)|}. \end{aligned}$$

4 Methodology

In this section, we propose a practical actor-critic algorithm that employs CSVE for value estimation and extends Advantage Weighted Regression[18] with out-of-sample state exploration for policy improvement. In particular, we adopt a dynamics model to sample OOD states during conservative value estimation and exploration during policy improvement. The implementation details are in Appendix B. Besides, we discuss the general technical choices of applying CSVE into algorithms.

4.1 Conservative Value Estimation

Given a dataset D acquired by the behavior policy π_β , our objective is to estimate the value function V^π for a target policy π . As stated in section 3, to prevent the value overestimation, we learn a conservative value function \hat{V}^π that lower bounds the real values of π by adding a penalty for OOD states within the Bellman projection sequence. Our method involves iterative updates of Equations 5 - 7, where \hat{Q}^k is the target network of \hat{Q}^k .

$$\hat{V}^{k+1} \leftarrow \arg \min_V L_V^\pi(V; \hat{Q}^k) \quad (5)$$

$$= \mathbb{E}_{s \sim D} \left[\left(\mathbb{E}_{a \sim \pi(\cdot|s)} [\hat{Q}^k(s, a)] - V(s) \right)^2 \right] + \alpha \left(\mathbb{E}_{s \sim D, a \sim \pi(\cdot|s)} [V(s')] - \mathbb{E}_{s \sim D} [V(s)] \right)_{s' \sim \hat{P}(s, a)}$$

$$\hat{Q}^{k+1} \leftarrow \arg \min_Q L_Q^\pi(Q; \hat{V}^{k+1}) = \mathbb{E}_{s, a, s' \sim D} \left[\left(r(s, a) + \gamma \hat{V}^{k+1}(s') - Q(s, a) \right)^2 \right] \quad (6)$$

$$\overline{\hat{Q}^{k+1}} \leftarrow (1 - \omega) \overline{\hat{Q}^k} + \omega \hat{Q}^{k+1} \quad (7)$$

The RHS of Eq. 5 is an approximation of Eq. 2, with the first term representing the standard TD error. In this term, the target state value is estimated by taking the expectation of $\overline{\hat{Q}^k}$ over $a \sim \pi$, and the second term penalizes the value of OOD states. In Eq. 6, the RHS is TD errors estimated on transitions in the dataset D . Note that the target term is the sum of the reward $r(s, a)$ and the next step state's value $\hat{V}^{k+1}(s')$. In Eq. 7, the target Q values are updated with a soft interpolation factor $\omega \in (0, 1)$. $\overline{\hat{Q}^k}$ changes slower than \hat{Q}^k , which makes the TD error estimation in Eq. 5 more stable.

Constrained Policy. Note that in RHS of Eq. 5, we use $a \sim \pi(\cdot|s)$ in expectation. To safely estimate the target value of $V(s)$ by $\mathbb{E}_{a \sim \pi(\cdot|s)} [\overline{\hat{Q}^k}(s, a)]$, we almost always requires $\text{supp}(\pi(\cdot|s)) \subset$

$\text{supp}(\pi_\beta(\cdot|s))$. We achieve this by the *advantage weighted policy update*, which forces $\pi(\cdot|s)$ to have significant probability mass on actions taken by π_β in data, as detailed in section 3.2.

Model-based OOD State Sampling. In Eq. 5, we implement the state sampling process $s' \sim d$ in Eq. 2 as a flow of $\{s \sim D; a \sim \pi(a|s), s' \sim \hat{P}(s'|s, a)\}$, that is the distribution of the predictive next-states from D by following π . This approach proves beneficial in practice. On the one hand, this method is more efficient as it samples only the states that are approximately reachable from D by one step, rather than sampling the entire state space. On the other hand, we only need the model to do one-step prediction such that it introduces no bootstrapped errors from long horizons. Following previous work [17, 15, 6], We use an ensemble of deep neural networks, represented as $p^{\theta^1}, \dots, p^{\theta^B}$, to implement the probabilistic dynamics model. Each neural network produces a Gaussian distribution over the next state and reward: $P_\theta^i(s_{t+1}, r|s_t, a_t) = \mathcal{N}(u_\theta^i(s_t, a_t), \sigma_\theta^i(s_t, a_t))$.

Adaptive Penalty Factor α . The pessimism level is controlled by the parameter $\alpha \geq 0$. In practice, we set α adaptive during training as follows, which is similar to that in CQL([4])

$$\max_{\alpha \geq 0} [\alpha (\mathbb{E}_{s' \sim d} [V_\psi(s')] - \mathbb{E}_{s \sim D} [V_\psi(s)] - \tau)], \quad (8)$$

where τ is a budget parameter. If the expected difference in V-values is less than τ , α will decrease. Otherwise, α will increase, penalizing the OOD state values more aggressively.

4.2 Advantage Weighted Policy Update

After learning the conservative \hat{V}^{k+1} and \hat{Q}^{k+1} (or \hat{V}^π and \hat{Q}^π when the values have converged), we improve the policy by the following advantage weighted update [12].

$$\pi \leftarrow \arg \min_{\pi'} L_\pi(\pi') = - \mathbb{E}_{s, a \sim D} \left[\log \pi'(a|s) \exp \left(\beta \hat{A}^{k+1}(s, a) \right) \right] \quad (9)$$

where $\hat{A}^{k+1}(s, a) = \hat{Q}^{k+1}(s, a) - \hat{V}^{k+1}(s)$. Eq.9 updates the policy π by applying a weighted maximum likelihood method. This is computed by re-weighting state-action samples in D using the estimated advantage \hat{A}^{k+1} . It avoids explicit estimation of the behavior policy, and its resulting sampling errors, which is an important issue in offline RL [12, 4].

Implicit policy constraints. We adopt the advantage-weighted policy update which imposes an implicit KL divergence constraint between π and π_β . This policy constraint is necessary to guarantee that the next state s' in Eq. 5 can be safely generated through policy π . As derived in [12] (Appendix A), Eq. 9 is a parametric solution of the following problem (where ϵ depends on β):

$$\begin{aligned} & \max_{\pi'} \mathbb{E}_{a \sim \pi'(\cdot|s)} [\hat{A}^{k+1}(s, a)] \\ & \text{s.t. } D_{\text{KL}}(\pi'(\cdot|s) \parallel \pi_\beta(\cdot|s)) \leq \epsilon, \quad \int_a \pi'(a|s) da = 1. \end{aligned}$$

Note that $D_{\text{KL}}(\pi' \parallel \pi_\beta)$ is a reserved KL divergence with respect to π' , which is mode-seeking [19]. When treated as Lagrangian it forces π' to allocate its probability mass to the maximum likelihood supports of π_β , re-weighted by the estimated advantage. In other words, for the space of A where $\pi_\beta(\cdot|s)$ has no samples, $\pi'(\cdot|s)$ has almost zero probability mass too.

Model-based Exploration on Near States. As suggested by remarks in Section 3.1, in practice, allowing the policy to explore the predicted next states transition ($s \sim D$) following $a \sim \pi'(\cdot|s)$ leads to better test performance. With this kind of exploration, the policy is updated as follows:

$$\pi \leftarrow \arg \min_{\pi'} L_\pi(\pi') - \lambda \mathbb{E}_{\substack{s \sim D, a \sim \pi'(s) \\ s' \sim \hat{P}(s, a)}} \left[r(s, a) + \gamma \hat{V}^{k+1}(s') \right]. \quad (10)$$

The second term is an approximation to $E_{s \sim d_\pi(s)} [V^\pi(s)]$. The optimization of this term involves calculating the gradient through the learned dynamics model. This is achieved by employing analytic gradients through the learned dynamics to maximize the value estimates. It is important to note that the value estimates rely on the reward and value predictions, which are dependent on the imagined states and actions. As all these steps are implemented using neural networks, the gradient is analytically computed using stochastic back-propagation, a concept inspired by Dreamer[20]. We adjust the value of λ , a hyper-parameter, to balance between optimistic policy optimization (in maximizing V) and the constrained policy update (as indicated by the first term).

Table 1: Performance comparison on Gym control tasks v2. The results of CSVE are over ten seeds and we reimplement AWAC using d3rlpy. Results of IQL, TD3-BC, and PBRL are from their original papers (Table 1 in [21], Table C.3 in [22], and Table 1 in [10] respectively). Results of COMBO and CQL are from the reproduction results in [23] (Table 1) and [10] respectively, since their original results were reported on v0 datasets.

		AWAC	CQL	CQL-AWR	COMBO	IQL	TD3-BC	PBRL	CSVE
Random	HalfCheetah	13.7	17.5 ± 1.5	16.9 ± 1.5	38.8	18.2	11.0 ± 1.1	13.1 ± 1.2	26.8 ± 1.5
	Hopper	8.7	7.9 ± 0.4	8.7 ± 0.5	17.9	16.3	8.5 ± 0.6	31.6 ± 0.3	26.1 ± 7.6
	Walker2D	2.2	5.1 ± 1.3	0.0 ± 1.6	7.0	5.5	1.6 ± 1.7	8.8 ± 6.3	6.2 ± 0.8
Medium	HalfCheetah	50.0	47.0 ± 0.5	50.9 ± 0.6	54.2	47.4	48.3 ± 0.3	58.2 ± 1.5	48.4 ± 0.3
	Hopper	97.5	53.0 ± 28.5	25.7 ± 37.4	94.9	66.3	59.3 ± 4.2	81.6 ± 14.5	96.7 ± 5.7
	Walker2D	89.1	73.3 ± 17.7	62.4 ± 24.4	75.5	78.3	83.7 ± 2.1	90.3 ± 1.2	83.2 ± 1.0
Medium Replay	HalfCheetah	44.9	45.5 ± 0.7	40.0 ± 0.4	55.1	44.2	44.6 ± 0.5	49.5 ± 0.8	54.5 ± 0.6
	Hopper	99.4	88.7 ± 12.9	91.0 ± 13.0	73.1	94.7	60.9 ± 18.8	100.7 ± 0.4	91.7 ± 0.2
	Walker2D	80.0	83.3 ± 2.7	66.7 ± 12.1	56.0	73.9	81.8 ± 5.5	86.2 ± 3.4	78.0 ± 1.5
Medium Expert	HalfCheetah	62.8	75.6 ± 25.7	73.4 ± 2.0	90.0	86.7	90.7 ± 4.3	93.1 ± 0.2	93.1 ± 0.3
	Hopper	87.2	105.6 ± 12.9	102.2 ± 7.7	111.1	91.5	98.0 ± 9.4	111.2 ± 0.7	94.1 ± 3.0
	Walker2D	109.8	107.9 ± 1.6	98.0 ± 21.7	96.1	109.6	110.1 ± 0.5	109.8 ± 0.2	109.0 ± 0.1
Expert	HalfCheetah	20.0	96.3 ± 1.3	87.3 ± 8.1	-	94.6	96.7 ± 1.1	96.2 ± 2.3	93.8 ± 0.1
	Hopper	111.6	96.5 ± 28.0	110.0 ± 2.5	-	109.0	107.8 ± 7	110.4 ± 0.3	111.3 ± 0.6
	Walker2D	110.6	108.5 ± 0.5	75.1 ± 60.7	-	109.4	110.2 ± 0.3	108.8 ± 0.2	108.5 ± 0.1
Average		65.8	67.4	60.6	64.1	69.7	67.5	76.7	74.8

4.3 Discussion on implementation choices

Now we examine the technical considerations for implementing CSVE in a practical algorithm.

Constraints on Policy Extraction. It is important to note that the state value function alone does not suffice to directly derive a policy. There are two methods for extracting a policy from CSVE. The first method is model-based planning, i.e., $\pi \leftarrow \arg \max_{\pi} \mathbb{E}_{s \sim d, a \sim \pi(\cdot|s)} [\hat{r}(s, a) + \gamma \mathbb{E}_{s' \sim \hat{P}(s, a)} [V(s')]]$, which involves finding the policy that maximizes the expected future return. However, this method heavily depends on the accuracy of a model and is difficult to implement in practice. As an alternative, we suggest the second method, which learns a Q value or advantage function from the V value function and experience data, and then extracts the policy. Note that CSVE provides no guarantees for conservative estimation on OOD actions, which can cause normal policy extraction methods such as SAC to fail. To address this issue, we adopt policy constraint techniques. On the one hand, during the value estimation in Eq.5, all current states are sampled from the dataset, while the policy is constrained to be close to the behavior policy (ensured via Eq.9). On the other hand, during the policy learning in Eq.10, we use AWR [18] as the primary policy extraction method (first term of Eq.10), which implicitly imposes policy constraints and the additional action exploration (second term of Eq.10) is strictly applied to states in the dataset. This exploration provides a bonus to actions that: (1) themselves and their model-predictive next-states are both close to the dataset (ensured by the dynamics model), and (2) their values are favorable even with conservatism.

Taking Advantage of CSVE. As outlined in Section 3.1, CSVE allows for a more relaxed lower bound on conservative value estimation compared to conservative Q values, providing greater potential for improving the policy. To take advantage of this, the algorithm should enable exploration of out-of-sample but in-distribution states, as described in Section 3. In this paper, we use a deep ensemble dynamics model to support this speculative state exploration, as shown in Eq. 10. The reasoning behind this is as follows: for an in-data state s and any action $a \sim \pi(\cdot|s)$, if the next state s' is in-data or close to the data support, its value is reasonably estimated, and if not, its value has been penalized according to Eq.5. Additionally, the deep ensemble dynamics model captures epistemic uncertainty well, which can effectively cancel out the impact of rare samples of s' . By utilizing CSVE, our algorithm can employ the speculative interpolation to further improve the policy. In contrast, CQL and AWAC do not have this capability for such enhanced policy optimization.

Table 2: Performance comparison on Adroit tasks. The results of CSVE are over ten seeds. Results of IQL are from Table 3 in [21] and results of other algorithms are from Table 4 in [10].

		AWAC	BC	BEAR	UWAC	CQL	CQL-AWR	IQL	PBRL	CSVE
Human	Pen	18.7	34.4	-1.0	10.1 ± 3.2	37.5	8.4 ± 7.1	71.5	35.4 ± 3.3	106.2 ± 5.0
	Hammer	-1.8	1.5	0.3	1.2 ± 0.7	4.4	0.3 ± 0.0	1.4	0.4 ± 0.3	3.5 ± 2.6
	Door	-1.8	0.5	-0.3	0.4 ± 0.2	9.9	3.5 ± 1.8	4.3	0.1 ± 0.0	2.8 ± 2.4
	Relocate	-0.1	0.0	-0.3	0.0 ± 0.0	0.2	0.1 ± 0.0	0.1	0.0 ± 0.0	0.1 ± 0.0
Cloned	Pen	27.2	56.9	26.5	23.0 ± 6.9	39.2	29.3 ± 7.1	37.3	74.9 ± 9.8	54.5 ± 5.4
	Hammer	-1.8	0.8	0.3	0.4 ± 0.0	2.1	0.31 ± 0.06	2.1	0.8 ± 0.5	0.5 ± 0.2
	Door	-2.1	-0.1	-0.1	0.0 ± 0.0	0.4	-0.2 ± 0.1	1.6	4.6 ± 4.8	1.2 ± 1.0
	Relocate	-0.4	-0.1	-0.3	-0.3 ± 0.2	-0.1	-0.3 ± 0.0	0.0	-0.1 ± 0.0	-0.3 ± 0.0
Expert	Pen	60.9	85.1	105.9	98.2 ± 9.1	107.0	47.1 ± 6.8	117.2	135.7 ± 3.4	144.0 ± 9.4
	Hammer	31.0	125.6	127.3	107.7 ± 21.7	86.7	0.2 ± 0.0	124.1	127.5 ± 0.2	126.5 ± 0.3
	Door	98.1	34.9	103.4	104.7 ± 0.4	101.5	85.0 ± 15.9	105.2	95.7 ± 12.2	104.2 ± 0.8
	Relocate	49.0	101.3	98.6	105.5 ± 3.2	95.0	7.2 ± 12.5	105.9	84.5 ± 12.2	102.9 ± 0.9
Average		23.1	36.7	38.4	37.6	40.3	15.1	47.6	46.6	53.8

5 Experiments

This section evaluates the effectiveness of our proposed CSVE algorithm for conservative value estimation in offline RL. In addition, we aim to compare the performance of CSVE with state-of-the-art (SOTA) algorithms. To achieve this, we conduct experimental evaluations on a variety of classic continuous control tasks of Gym[7] and Adroit[8] in the D4RL[9] benchmark.

Our compared baselines include: (1) CQL[4] and its variants, CQL-AWR (Appendix D.2) which uses AWR with extra in-sample exploration as policy extractor, COMBO[6] which extends CQL with model-based rollouts; (2) AWR variants, including AWAC[12] which is a special case of our algorithm with no value penalization (i.e., $d = d_u$ in Eq. 2) and exploration on OOD states, IQL[21] which adopts expectile-based conservative value estimation; (3) PBRL[10], a strong algorithm in offline RL, but is quite costly on computation since it uses the ensemble of hundreds of sub-models; (4) other SOTA algorithms with public performance results or high-quality open source implementations, including TD3-BC[22], UWAC[24] and BEAR[25]). Comparing with CQL variants allows us to investigate the advantages of conservative estimation on state values over Q values. By comparing with AWR variants, we distinguish the performance contribution of CSVE from the AWR policy extraction used in our implementation.

5.1 Overall Performance

Evaluation on the Gym Control Tasks. Our method, CSVE, was trained for 1 million steps and evaluated. The results are shown in Table 1. Compared to CQL, CSVE outperforms it in 11 out of 15 tasks, with similar performance on the remaining tasks. Additionally, CSVE shows a consistent advantage on datasets that were generated by following random or sub-optimal policies (random and medium). The CQL-AWR method showed slight improvement in some cases, but still underperforms compared to CSVE. When compared to COMBO, CSVE performs better in 7 out of 12 tasks and similarly or slightly worse on the remaining tasks, which highlights the effectiveness of our method’s better bounds on V . Our method has a clear advantage in extracting the best policy on medium and medium-expert tasks. Overall, our results provide empirical evidence that using conservative value estimation on states, rather than Q, leads to improved performance in offline RL. CSVE outperforms AWAC in 9 out of 15 tasks, demonstrating the effectiveness of our approach in exploring beyond the behavior policy. Additionally, our method excels in extracting the optimal policy on data with mixed policies (medium-expert) where AWAC falls short. In comparison to IQL, our method achieves higher scores in 7 out of 9 tasks and maintains comparable performance in the remaining tasks. Furthermore, despite having a significantly lower model capacity and computation cost, CSVE outperforms TD3-BC and is on par with PBRL. These results highlight the effectiveness of our conservative value estimation approach.

Evaluation on the Adroit Tasks. In Table 2, we report the final evaluation results after training 0.1 million steps. As shown, our method outperforms IQL in 8 out of 12 tasks, and is competitive with other algorithms on expert datasets. Additionally, we note that CSVE is the only method that

can learn an effective policy on the human dataset for the Pen task, while maintaining medium performance on the cloned dataset. Overall, our results empirically support the effectiveness of our proposed tighter conservative value estimation in improving offline RL performance.

5.2 Ablation Study

Effect of Exploration on Near States. We analyze the impact of varying the factor λ in Eq. 10, which controls the intensity on such exploration. We investigated λ values of $\{0.0, 0.1, 0.5, 1.0\}$ in the medium tasks, fixing $\beta = 0.1$. The results are plotted in Fig. 1. As shown in the upper figures, λ has an obvious effect on policy performance and variances during training. With increasing λ from 0, the converged performance gets better in general. However, when the value of λ becomes too large (e.g., $\lambda = 3$ for hopper and walker2d), the performance may degrade or even collapse. We further investigated the L_π loss as depicted in the bottom figures of Eq. 9, finding that larger λ values negatively impact L_π ; however, once L_π converges to a reasonable low value, larger λ values lead to performance improvement.

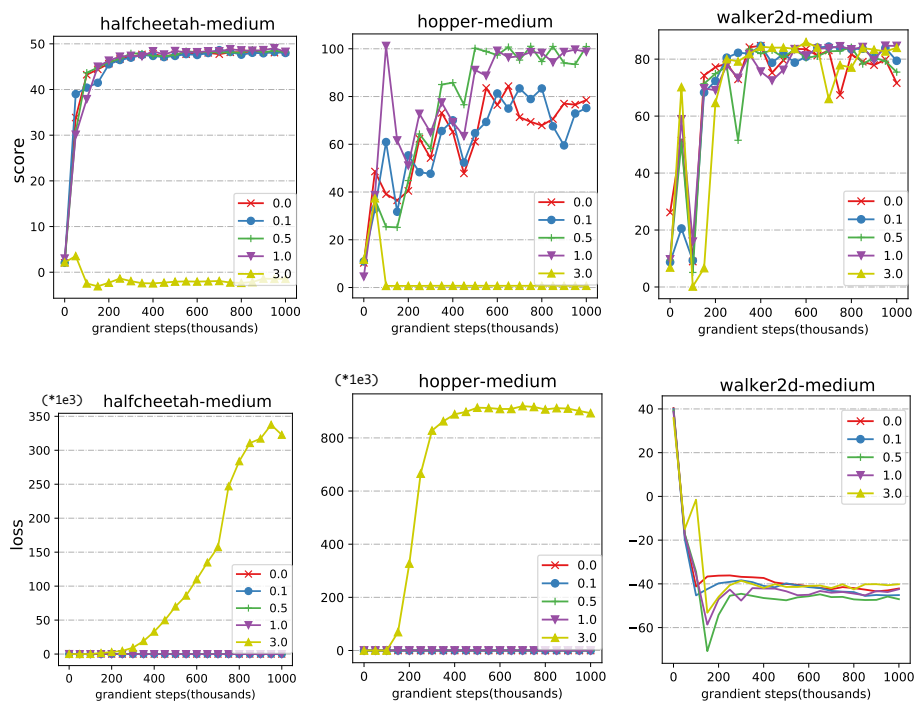


Figure 1: Effect of λ to performance scores (upper figures) and L_π losses (bottom figures) in Eq. 9 on medium tasks.

Effect of In-sample Policy Optimization. We examined the impact of varying the factor β in Eq. 9 on the balance between behavior cloning and in-sample policy optimization. We tested different β values on mujoco medium datasets, as shown in Fig.2. The results indicate that β has a significant effect on the policy performance during training. Based on our findings, a value of $\beta = 3.0$ was found to be suitable for medium datasets. Additionally, in our implementation, we use $\beta = 3.0$ for random and medium tasks, and $\beta = 0.1$ for medium-replay, medium-expert, and expert datasets. More details can be found in the ablation study in the appendix.

6 Related work

The main idea behind offline RL algorithms is to incorporate conservatism or regularization into the online RL algorithms. Here, we briefly review prior work and compare it to our approach.

Conservative Value Estimation: Prior offline RL algorithms regularize the learning policy to be close to the data or to an explicitly estimated behavior policy. and penalize the exploration

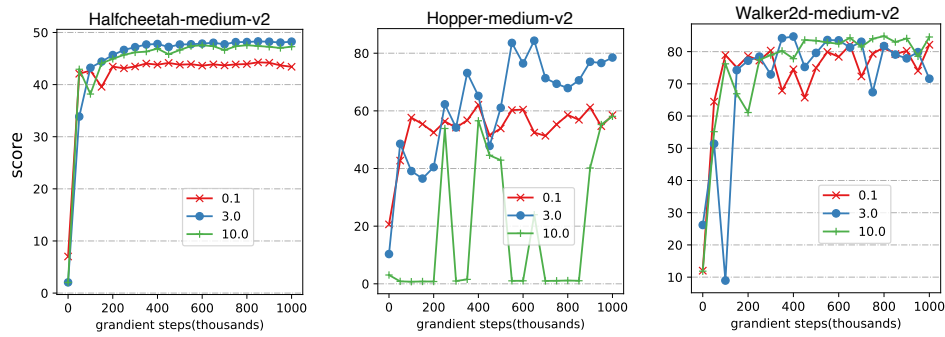


Figure 2: Effect of β to performance scores on medium tasks.

of the OOD region, via distribution correction estimation [26, 27], policy constraints with support matching [11] and distributional matching [1, 25], applying policy divergence based penalty on Q-functions [28, 29] or uncertainty-based penalty [30] on Q-functions and conservative Q-function estimation [4]. Besides, model-based algorithms [15] directly estimate dynamics uncertainty and translate it into reward penalty. Different from this prior work that imposes conservatism on state-action pairs or actions, ours directly does such conservative estimation on states and requires no explicit uncertainty quantification.

In-Sample Algorithms: AWR [18] updates policy constrained on strictly in-sample states and actions, to avoid extrapolation on out-of-support points. IQL[21] uses expectile-based regression to do value estimation and AWR for its policy updates. AWAC[12], whose actor is AWR, is an actor-critic algorithm to accelerate online RL with offline data. The major drawback of AWR method when used for offline RL is that the in-sample policy learning limits the final performance.

Model-Based Algorithms: Model-based offline RL learns the dynamics model from the static dataset and uses it to quantify uncertainty [15], data augmentation [6] with roll-outs, or planning [16, 31]. Such methods typically rely on wide data coverage when planning and data augmentation with roll-outs, and low model estimation error when estimating uncertainty, which is difficult to satisfy in reality and leads to policy instability. Instead, we use the model to sample the next-step states only reachable from data, which has no such strict requirements on data coverage or model bias.

Theoretical Results: Our theoretical results are derived from conservative Q-value estimation (CQL) and safe policy improvement [32]. Compared to offline policy evaluation[33], which aims to provide a better estimation of the value function, we focus on providing a better lower bound. Additionally, when the dataset is augmented with model-based roll-outs, COMBO [6] provides a more conservative yet tighter value estimation than CQL. CSVE achieves the same lower bounds as COMBO but under more general state distributions.

7 Conclusions

In this paper, we propose CSVE, a new approach for offline RL based on conservative value estimation on states. We demonstrated how its theoretical results can lead to more effective algorithms. In particular, we develop a practical actor-critic algorithm, in which the critic achieves conservative state value estimation by incorporating the penalty of the model predictive next-states into Bellman iterations, and the actor does the advantage-weighted policy updates enhanced via model-based state exploration. Experimental evaluation shows that our method performs better than alternative methods based on conservative Q-function estimation and is competitive among the SOTA methods, thereby validating our theoretical analysis. Moving forward, we aim to delve deeper into designing more powerful algorithms grounded in conservative state value estimation.

References

- [1] Scott Fujimoto, David Meger, and Doina Precup. Off-policy deep reinforcement learning without exploration. In Kamalika Chaudhuri and Ruslan Salakhutdinov, editors, *Proceedings of the 36th International Conference on Machine Learning*, volume 97 of *Proceedings of Machine Learning Research*, pages 2052–2062. PMLR, 09–15 Jun 2019.
- [2] Sascha Lange, Thomas Gabel, and Martin Riedmiller. Batch reinforcement learning. In *Reinforcement learning*, pages 45–73. Springer, 2012.
- [3] Laixi Shi, Gen Li, Yuting Wei, Yuxin Chen, and Yuejie Chi. Pessimistic q-learning for offline reinforcement learning: Towards optimal sample complexity. In Kamalika Chaudhuri, Stefanie Jegelka, Le Song, Csaba Szepesvari, Gang Niu, and Sivan Sabato, editors, *Proceedings of the 39th International Conference on Machine Learning*, volume 162 of *Proceedings of Machine Learning Research*, pages 19967–20025. PMLR, 17–23 Jul 2022.
- [4] Aviral Kumar, Aurick Zhou, George Tucker, and Sergey Levine. Conservative q-learning for offline reinforcement learning. *Advances in Neural Information Processing Systems*, 33:1179–1191, 2020.
- [5] Jacob Buckman, Carles Gelada, and Marc G Bellemare. The importance of pessimism in fixed-dataset policy optimization. In *International Conference on Learning Representations*, 2020.
- [6] Tianhe Yu, Aviral Kumar, Rafael Rafailov, Aravind Rajeswaran, Sergey Levine, and Chelsea Finn. Combo: Conservative offline model-based policy optimization. *Advances in neural information processing systems*, 34:28954–28967, 2021.
- [7] Greg Brockman, Vicki Cheung, Ludwig Pettersson, Jonas Schneider, John Schulman, Jie Tang, and Wojciech Zaremba. Openai gym. *arXiv preprint arXiv:1606.01540*, 2016.
- [8] Aravind Rajeswaran, Vikash Kumar, Abhishek Gupta, Giulia Vezzani, John Schulman, Emanuel Todorov, and Sergey Levine. Learning complex dexterous manipulation with deep reinforcement learning and demonstrations. *arXiv preprint arXiv:1709.10087*, 2017.
- [9] Justin Fu, Aviral Kumar, Ofir Nachum, George Tucker, and Sergey Levine. D4rl: Datasets for deep data-driven reinforcement learning. *arXiv preprint arXiv:2004.07219*, 2020.
- [10] Chenjia Bai, Lingxiao Wang, Zhuoran Yang, Zhi-Hong Deng, Animesh Garg, Peng Liu, and Zhaoran Wang. Pessimistic bootstrapping for uncertainty-driven offline reinforcement learning. In *International Conference on Learning Representations*, 2021.
- [11] Yifan Wu, George Tucker, and Ofir Nachum. Behavior regularized offline reinforcement learning. *arXiv preprint arXiv:1911.11361*, 2019.
- [12] Ashvin Nair, Abhishek Gupta, Murtaza Dalal, and Sergey Levine. Awac: Accelerating online reinforcement learning with offline datasets, 2020.
- [13] Sergey Levine, Aviral Kumar, George Tucker, and Justin Fu. Offline reinforcement learning: Tutorial, review, and perspectives on open problems, 2020.
- [14] Xue Bin Peng, Aviral Kumar, Grace Zhang, and Sergey Levine. Advantage-weighted regression: Simple and scalable off-policy reinforcement learning. *arXiv preprint arXiv:1910.00177*, 2019.
- [15] Tianhe Yu, Garrett Thomas, Lantao Yu, Stefano Ermon, James Y Zou, Sergey Levine, Chelsea Finn, and Tengyu Ma. Mopo: Model-based offline policy optimization. *Advances in Neural Information Processing Systems*, 33:14129–14142, 2020.
- [16] Rahul Kidambi, Aravind Rajeswaran, Praneeth Netrapalli, and Thorsten Joachims. Morel: Model-based offline reinforcement learning. *Advances in neural information processing systems*, 33:21810–21823, 2020.
- [17] Michael Janner, Justin Fu, Marvin Zhang, and Sergey Levine. When to trust your model: Model-based policy optimization. *Advances in Neural Information Processing Systems*, 32, 2019.

- [18] Xue Bin Peng, Aviral Kumar, Grace Zhang, and Sergey Levine. Advantage-weighted regression: Simple and scalable off-policy reinforcement learning. *CoRR*, abs/1910.00177, 2019.
- [19] Jonathon Shlens. Notes on kullback-leibler divergence and likelihood. *CoRR*, abs/1404.2000, 2014.
- [20] Danijar Hafner, Timothy Lillicrap, Jimmy Ba, and Mohammad Norouzi. Dream to control: Learning behaviors by latent imagination. *arXiv preprint arXiv:1912.01603*, 2019.
- [21] Ilya Kostrikov, Ashvin Nair, and Sergey Levine. Offline reinforcement learning with implicit q-learning. In *International Conference on Learning Representations*, 2021.
- [22] Scott Fujimoto and Shixiang Shane Gu. A minimalist approach to offline reinforcement learning. *Advances in neural information processing systems*, 34:20132–20145, 2021.
- [23] Marc Rigter, Bruno Lacerda, and Nick Hawes. Rambo-rl: Robust adversarial model-based offline reinforcement learning. *Advances in Neural Information Processing Systems*, 2022.
- [24] Yue Wu, Shuangfei Zhai, Nitish Srivastava, Joshua Susskind, Jian Zhang, Ruslan Salakhutdinov, and Hanlin Goh. Uncertainty weighted actor-critic for offline reinforcement learning. *arXiv preprint arXiv:2105.08140*, 2021.
- [25] Aviral Kumar, Justin Fu, Matthew Soh, George Tucker, and Sergey Levine. Stabilizing off-policy q-learning via bootstrapping error reduction. *Advances in Neural Information Processing Systems*, 32, 2019.
- [26] Bo Dai, Ofir Nachum, Yinlam Chow, Lihong Li, Csaba Szepesvári, and Dale Schuurmans. Coincide: Off-policy confidence interval estimation. *Advances in neural information processing systems*, 33:9398–9411, 2020.
- [27] Mengjiao Yang, Ofir Nachum, Bo Dai, Lihong Li, and Dale Schuurmans. Off-policy evaluation via the regularized lagrangian. *Advances in Neural Information Processing Systems*, 33:6551–6561, 2020.
- [28] Ilya Kostrikov, Rob Fergus, Jonathan Tompson, and Ofir Nachum. Offline reinforcement learning with fisher divergence critic regularization. In *International Conference on Machine Learning*, pages 5774–5783. PMLR, 2021.
- [29] Ziyu Wang, Alexander Novikov, Konrad Zolna, Josh S Merel, Jost Tobias Springenberg, Scott E Reed, Bobak Shahriari, Noah Siegel, Caglar Gulcehre, Nicolas Heess, et al. Critic regularized regression. *Advances in Neural Information Processing Systems*, 33:7768–7778, 2020.
- [30] Rishabh Agarwal, Dale Schuurmans, and Mohammad Norouzi. An optimistic perspective on offline reinforcement learning. In *International Conference on Machine Learning*, pages 104–114. PMLR, 2020.
- [31] Xiong-Hui Chen, Yang Yu, Qingyang Li, Fan-Ming Luo, Zhiwei Qin, Wenjie Shang, and Jieping Ye. Offline model-based adaptable policy learning. *Advances in Neural Information Processing Systems*, 34:8432–8443, 2021.
- [32] Romain Laroche, Paul Trichelair, and Remi Tachet Des Combes. Safe policy improvement with baseline bootstrapping. In *International Conference on Machine Learning*, pages 3652–3661. PMLR, 2019.
- [33] Carles Gelada and Marc G Bellemare. Off-policy deep reinforcement learning by bootstrapping the covariate shift. In *Proceedings of the AAAI Conference on Artificial Intelligence*, volume 33, pages 3647–3655, 2019.
- [34] Takuma Seno and Michita Imai. d3rlpy: An offline deep reinforcement learning library. *arXiv preprint arXiv:2111.03788*, 2021.
- [35] Yuwei Fu, Di Wu, and Benoit Boulet. A closer look at offline rl agents. In *Advances in Neural Information Processing Systems*, 2022.

A Proofs

We first redefine notation for clarity and then provide the proofs of the results from the main paper.

Notation. Let $k \in N$ denotes an iteration of policy evaluation(in Section 3.2). V^k denotes the true, tabular (or functional) V-function iterate in the MDP. \hat{V}^k denotes the approximate tabular (or functional) V-function iterate.

The empirical Bellman operator is defined as:

$$(\hat{\mathcal{B}}^\pi \hat{V}^k)(s) = E_{a \sim \pi(a|s)} \hat{r}(s, a) + \gamma \sum_{s'} E_{a \sim \pi(a|s)} \hat{P}(s'|s, a) [\hat{V}^k(s')] \quad (11)$$

where $\hat{r}(s, a)$ is the empirical average reward derived from the dataset when performing action a at state s . The true Bellman operator is given by:

$$(\mathcal{B}^\pi V^k)(s) = E_{a \sim \pi(a|s)} r(s, a) + \gamma \sum_{s'} E_{a \sim \pi(a|s)} P(s'|s, a) [V^k(s')] \quad (12)$$

Now we first prove that the iteration in Eq.2 has a fixed point. Assume the state value function is lower bounded, i.e., $V(s) \geq C \forall s \in S$, then Eq.2 can always be solved with Eq.3. Thus, we only need to investigate the iteration in Eq.3.

Defining this iteration as a function operator \mathcal{T}^π on V and supposing that $\text{supp } d \subseteq \text{supp } d_u$, it's evident that the operator \mathcal{T}^π displays a γ -contraction within L_∞ norm where γ is the discounting factor.

Proof of Lemma 3.1: Let V and V' be any two state value functions with the same support, i.e., $\text{supp } V = \text{supp } V'$.

$$\begin{aligned} |(\mathcal{T}^\pi V - \mathcal{T}^\pi V')(s)| &= \left| (\hat{\mathcal{B}}^\pi V(s) - \alpha \left[\frac{d(s)}{d_u(s)} - 1 \right]) - (\hat{\mathcal{B}}^\pi V'(s) - \alpha \left[\frac{d(s)}{d_u(s)} - 1 \right]) \right| \\ &= \left| \hat{\mathcal{B}}^\pi V(s) - \hat{\mathcal{B}}^\pi V'(s) \right| \\ &= | (E_{a \sim \pi(a|s)} \hat{r}(s, a) + \gamma E_{a \sim \pi(a|s)} \sum_{s'} \hat{P}(s'|s, a) V(s')) \\ &\quad - (E_{a \sim \pi(a|s)} \hat{r}(s, a) + \gamma E_{a \sim \pi(a|s)} \sum_{s'} \hat{P}(s'|s, a) V'(s')) | \\ &= \gamma \left| E_{a \sim \pi(a|s)} \sum_{s'} \hat{P}(s'|s, a) [V(s') - V'(s')] \right| \end{aligned}$$

$$\begin{aligned} \|\mathcal{T}^\pi V - \mathcal{T}^\pi V'\|_\infty &= \max_s |(\mathcal{T}^\pi V - \mathcal{T}^\pi V')(s)| \\ &= \max_s \gamma \left| E_{a \sim \pi(a|s)} \sum_{s'} \hat{P}(s'|s, a) [V(s') - V'(s')] \right| \\ &\leq \gamma E_{a \sim \pi(a|s)} \sum_{s'} \hat{P}(s'|s, a) \max_{s''} |V(s'') - V'(s'')| \\ &= \gamma \max_{s''} |V(s'') - V'(s'')| \\ &= \gamma \| (V - V') \|_\infty \end{aligned}$$

□

We provide a bound on the difference between the empirical Bellman operator and the true Bellman operator. Following previous work [4], we make the following assumptions. Let P^π be the transition matrix associated with the policy, specifically, $P^\pi V(s) = E_{a' \sim \pi(a'|s), s' \sim P(s'|s, a')} [V(s')]$

Assumption A.1. $\forall s, a \in \mathcal{M}$, the relationship below hold with at least a $(1 - \delta)$ ($\delta \in (0, 1)$) probability,

$$|r - r(s, a)| \leq \frac{C_{r,\delta}}{\sqrt{|D(s, a)|}}, \|\hat{P}(s'|s, a) - P(s'|s, a)\|_1 \leq \frac{C_{P,\delta}}{\sqrt{|D(s, a)|}} \quad (13)$$

Given this assumption, the absolute difference between the empirical Bellman operator and the true one can be deduced as follows:

$$|(\hat{\mathcal{B}}^\pi)\hat{V}^k - (\mathcal{B}^\pi)\hat{V}^k| = E_{a \sim \pi(a|s)}|r - r(s, a) + \gamma \sum_{s'} E_{a' \sim \pi(a'|s')}(\hat{P}(s'|s, a) - P(s'|s, a))[\hat{V}^k(s')]| \quad (14)$$

$$\leq E_{a \sim \pi(a|s)}|r - r(s, a)| + \gamma \left| \sum_{s'} E_{a' \sim \pi(a'|s')}(\hat{P}(s'|s, a') - P(s'|s, a'))[\hat{V}^k(s')] \right| \quad (15)$$

$$\leq E_{a \sim \pi(a|s)} \frac{C_{r,\delta} + \gamma C_{P,\delta} 2R_{max}/(1 - \gamma)}{\sqrt{|D(s, a)|}} \quad (16)$$

The error in estimation due to sampling can therefore be bounded by a constant, dependent on $C_{r,\delta}$ and $C_{t,\delta}$. We define this constant as $C_{r,T,\delta}$.

Thus we obtain:

$$\forall V, s \in D, |\hat{\mathcal{B}}^\pi V(s) - \mathcal{B}^\pi V(s)| \leq E_{a \sim \pi(a|s)} \frac{C_{r,t,\delta}}{(1 - \gamma)\sqrt{|D(s, a)|}} \quad (17)$$

Next we provide an important lemma.

Lemma A.2. (Interpolation Lemma) For any $f \in [0, 1]$, and any given distribution $\rho(s)$, let d_f be an f -interpolation of ρ and D , i.e., $d_f(s) := fd(s) + (1 - f)\rho(s)$, let $v(\rho, f) := E_{s \sim \rho(s)}[\frac{\rho(s) - d_f(s)}{d_f(s)}]$, then $v(\rho, f)$ satisfies $v(\rho, f) \geq 0$.

The proof can be found in [6]. By setting f as 1, we have $E_{s \sim \rho(s)}[\frac{\rho(s) - d(s)}{d(s)}] > 0$.

Proof of Theorem 3.2: The V function of approximate dynamic programming in iteration k can be obtained as:

$$\hat{V}^{k+1}(s) = \hat{\mathcal{B}}^\pi \hat{V}^k(s) - \alpha \left[\frac{d(s)}{d_u(s)} - 1 \right] \forall s, k \quad (18)$$

The fixed point:

$$\hat{V}^\pi(s) = \hat{\mathcal{B}}^\pi \hat{V}^\pi(s) - \alpha \left[\frac{d(s)}{d_u(s)} - 1 \right] \leq \mathcal{B}^\pi \hat{V}^\pi(s) + E_{a \sim \pi(a|s)} \frac{C_{r,t,\delta} R_{max}}{(1 - \gamma)\sqrt{|D(s, a)|}} - \alpha \left[\frac{d(s)}{d_u(s)} - 1 \right] \quad (19)$$

Thus we obtain:

$$\hat{V}^\pi(s) \leq V^\pi(s) + (I - \gamma P^\pi)^{-1} E_{a \sim \pi(a|s)} \frac{C_{r,t,\delta} R_{max}}{(1 - \gamma)\sqrt{|D(s, a)|}} - \alpha (I - \gamma P^\pi)^{-1} \left[\frac{d(s)}{d_u(s)} - 1 \right] \quad (20)$$

, where P^π is the transition matrix coupled with the policy π and $P^\pi V(s) = E_{a' \sim \pi(a'|s') s' \sim P(s'|s, a')} [V(s')]$.

Then the expectation of $V^\pi(s)$ under distribution $d(s)$ satisfies:

$$E_{s \sim d(s)} \hat{V}^\pi(s) \leq E_{s \sim d(s)} (V^\pi(s)) + E_{s \sim d(s)} (I - \gamma P^\pi)^{-1} E_{a \sim \pi(a|s)} \frac{C_{r,t,\delta} R_{max}}{(1 - \gamma)\sqrt{|D(s, a)|}} - \underbrace{\alpha E_{s \sim d(s)} (I - \gamma P^\pi)^{-1} \left[\frac{d(s)}{d_u(s)} - 1 \right]}_{>0} \quad (21)$$

When $\alpha \geq \frac{E_{s \sim d(s)} E_{a \sim \pi(a|s)} \frac{C_{r,t,\delta} R_{max}}{(1-\gamma)\sqrt{|D(s,a)|}}}{E_{s \sim d(s)} [\frac{d(s)}{d_u(s)} - 1]}$, $E_{s \sim d(s)} \hat{V}^\pi(s) \leq E_{s \sim d(s)} (V^\pi(s))$. \square

Proof of Theorem 3.3: The expectation of $V^\pi(s)$ under distribution $d(s)$ satisfies:

$$E_{s \sim d_u(s)} \hat{V}^\pi(s) \leq E_{s \sim d_u(s)} (V^\pi(s)) + E_{s \sim d_u(s)} (I - \gamma P^\pi)^{-1} E_{a \sim \pi(a|s)} \frac{C_{r,t,\delta} R_{max}}{(1-\gamma)\sqrt{|D(s,a)|}} - \alpha E_{s \sim d_u(s)} (I - \gamma P^\pi)^{-1} [\frac{d(s)}{d_u(s)} - 1] \quad (22)$$

Noticed that the last term:

$$\sum_{s \sim d_u(s)} (\frac{d_f(s)}{d_u(s)} - 1) = \sum_s d_u(s) (\frac{d_f(s)}{d_u(s)} - 1) = \sum_s d_f(s) - \sum_s d_u(s) = 0 \quad (23)$$

We obtain that:

$$E_{s \sim d_u(s)} \hat{V}^\pi(s) \leq E_{s \sim d_u(s)} (V^\pi(s)) + E_{s \sim d_u(s)} (I - \gamma P^\pi)^{-1} E_{a \sim \pi(a|s)} \frac{C_{r,t,\delta} R_{max}}{(1-\gamma)\sqrt{|D(s,a)|}} \quad (24)$$

\square

Proof of Theorem 3.4: Recall that the expression of the V-function iterate is given by:

$$\hat{V}^{k+1}(s) = \mathcal{B}^{\pi^k} \hat{V}^k(s) - \alpha [\frac{d(s)}{d_u(s)} - 1] \forall s, k \quad (25)$$

Now the expectation of $V^\pi(s)$ under distribution $d_u(s)$ is given by:

$$E_{s \sim d_u(s)} \hat{V}^{k+1}(s) = E_{s \sim d_u(s)} \left[\mathcal{B}^{\pi^k} \hat{V}^k(s) - \alpha [\frac{d(s)}{d_u(s)} - 1] \right] = E_{s \sim d_u(s)} \mathcal{B}^{\pi^k} \hat{V}^k(s) \quad (26)$$

The expectation of $V^\pi(s)$ under distribution $d(s)$ is given by:

$$E_{s \sim d(s)} \hat{V}^{k+1}(s) = E_{s \sim d(s)} \mathcal{B}^{\pi^k} \hat{V}^k(s) - \alpha [\frac{d(s)}{d_u(s)} - 1] = E_{s \sim d(s)} \mathcal{B}^{\pi^k} \hat{V}^k(s) - \alpha E_{s \sim d(s)} [\frac{d(s)}{d_u(s)} - 1] \quad (27)$$

Thus we can show that:

$$\begin{aligned} E_{s \sim d_u(s)} \hat{V}^{k+1}(s) - E_{s \sim d(s)} \hat{V}^{k+1}(s) &= E_{s \sim d_u(s)} \mathcal{B}^{\pi^k} \hat{V}^k(s) - E_{s \sim d(s)} \mathcal{B}^{\pi^k} \hat{V}^k(s) + \alpha E_{s \sim d(s)} [\frac{d(s)}{d_u(s)} - 1] \\ &= E_{s \sim d_u(s)} V^{k+1}(s) - E_{s \sim d(s)} V^{k+1}(s) - E_{s \sim d(s)} [\mathcal{B}^{\pi^k} (\hat{V}^k - V^k)] \\ &\quad + E_{s \sim d_u(s)} [\mathcal{B}^{\pi^k} (\hat{V}^k - V^k)] + \alpha E_{s \sim d(s)} [\frac{d(s)}{d_u(s)} - 1] \end{aligned} \quad (28)$$

By choosing α :

$$\alpha > \frac{E_{s \sim d(s)} [\mathcal{B}^{\pi^k} (\hat{V}^k - V^k)] - E_{s \sim d_u(s)} [\mathcal{B}^{\pi^k} (\hat{V}^k - V^k)]}{E_{s \sim d(s)} [\frac{d(s)}{d_u(s)} - 1]} \quad (29)$$

We have $E_{s \sim d_u(s)} \hat{V}^{k+1}(s) - E_{s \sim d(s)} \hat{V}^{k+1}(s) > E_{s \sim d_u(s)} V^{k+1}(s) - E_{s \sim d(s)} V^{k+1}(s)$ hold. \square

Proof of Theorem 3.5: \hat{V} is obtained by solving the recursive Bellman fixed point equation in the empirical MDP, with an altered reward, $r(s, a) - \alpha [\frac{d(s)}{d_u(s)} - 1]$, hence the optimal policy $\pi^*(a|s)$ obtained by optimizing the value under Eq. 3.5. \square

Proof of Theorem 3.6: The proof of this statement is divided into two parts. We first relates the return of π^* in the empirical MDP \hat{M} with the return of π_β , we can get:

$$J(\pi^*, \hat{M}) - \alpha \frac{1}{1-\gamma} \mathbb{E}_{s \sim d_{\hat{M}}^{\pi^*}(s)} [\frac{d(s)}{d_u(s)} - 1] \geq J(\pi_\beta, \hat{M}) - 0 = J(\pi_\beta, \hat{M}) \quad (30)$$

Algorithm 1 CSVE based Offline RL Algorithm

Input: data $D = \{(s, a, r, s')\}$

Parametered Models: $Q_\theta, V_\psi, \pi_\phi, \bar{Q}_{\bar{\theta}}, M_\nu$

Hyperparameters: α, λ , learning rates $\eta_\theta, \eta_\psi, \eta_\phi, \omega$

▷ Train the transition model with the static dataset D

$M_\nu \leftarrow \text{train}(D)$.

▷ Train the conservative value estimation and policy functions

Initialize function parameters $\theta_0, \psi_0, \phi_0, \bar{\theta}_0 = \theta_0$

for step $k = 1$ **to** N **do**

$$\psi_k \leftarrow \psi_{k-1} - \eta_\psi \nabla_{\psi} L_V^\pi(V_\psi; \bar{Q}_{\theta_k})$$

$$\theta_k \leftarrow \theta_{k-1} - \eta_\theta \nabla_{\theta} L_Q^\pi(Q_\theta; \hat{V}_{\psi_k})$$

$$\phi_k \leftarrow \phi_{k-1} - \eta_\phi \nabla_{\phi} L_\pi^+(\pi_\phi)$$

$$\bar{\theta}_k \leftarrow \omega \bar{\theta}_{k-1} + (1 - \omega) \theta_k$$

end for

The next step is to bound the difference between $J(\pi_\beta, \hat{M})$ and $J(\pi_\beta, M)$ and the difference between $J(\pi^*, \hat{M})$ and $J(\pi^*, M)$. We quote a useful lemma from [4] (Lemma D.4.1):

Lemma A.3. For any MDP M , an empirical MDP \hat{M} generated by sampling actions according to the behavior policy π_β and a given policy π ,

$$|J(\pi, \hat{M}) - J(\pi, M)| \leq \left(\frac{C_{r,\delta}}{1-\gamma} + \frac{\gamma R_{max} C_{T,\delta}}{(1-\gamma)^2} \right) \mathbb{E}_{s \sim d_{\hat{M}}^{\pi^*}(s)} \left[\frac{\sqrt{|\mathcal{A}|}}{\sqrt{|\mathcal{D}(s)|}} \sqrt{E_{a \sim \pi(a|s)} \left(\frac{\pi(a|s)}{\pi_\beta(a|s)} \right)} \right] \quad (31)$$

Setting π in the above lemma as π_β , we get:

$$|J(\pi_\beta, \hat{M}) - J(\pi_\beta, M)| \leq \left(\frac{C_{r,\delta}}{1-\gamma} + \frac{\gamma R_{max} C_{T,\delta}}{(1-\gamma)^2} \right) \mathbb{E}_{s \sim d_{\hat{M}}^{\pi^*}(s)} \left[\frac{\sqrt{|\mathcal{A}|}}{\sqrt{|\mathcal{D}(s)|}} \sqrt{E_{a \sim \pi^*(a|s)} \left(\frac{\pi^*(a|s)}{\pi_\beta(a|s)} \right)} \right] \quad (32)$$

given that $\sqrt{E_{a \sim \pi^*(a|s)} \left[\frac{\pi^*(a|s)}{\pi_\beta(a|s)} \right]}$ is a pointwise upper bound of $\sqrt{E_{a \sim \pi_\beta(a|s)} \left[\frac{\pi_\beta(a|s)}{\pi_\beta(a|s)} \right]}$ ([4]). Thus we get,

$$\begin{aligned} J(\pi^*, \hat{M}) &\geq J(\pi_\beta, \hat{M}) - 2 \left(\frac{C_{r,\delta}}{1-\gamma} + \frac{\gamma R_{max} C_{T,\delta}}{(1-\gamma)^2} \right) \mathbb{E}_{s \sim d_{\hat{M}}^{\pi^*}(s)} \left[\frac{\sqrt{|\mathcal{A}|}}{\sqrt{|\mathcal{D}(s)|}} \sqrt{E_{a \sim \pi^*(a|s)} \left(\frac{\pi^*(a|s)}{\pi_\beta(a|s)} \right)} \right] \\ &\quad + \alpha \frac{1}{1-\gamma} \mathbb{E}_{s \sim d_{\hat{M}}^{\pi^*}(s)} \left[\frac{d(s)}{d_u(s)} - 1 \right] \end{aligned} \quad (33)$$

which completes the proof. \square

Here, the second term represents the sampling error, which arises due to the discrepancy between \hat{M} and M . The third term signifies the enhancement in policy performance attributed to our algorithm in \hat{M} . It's worth noting that when the first term is minimized, smaller values of α can achieve improvements over the behavior policy.

B CSVE Algorithm and Implementation Details

In Section 4, we detailed the complete formula descriptions of the CSVE practical offline RL algorithm. Here we consolidate those details and present the full deep offline reinforcement learning algorithm as illustrated in Alg. 1. In particular, the dynamic model, value functions, and policy are parameterized with deep neural networks and optimized via stochastic gradient descent methods.

We implement our method based on an offline deep reinforcement learning library d3rlpy [34]. The code is available at: <https://github.com/2023AnonymousAuthor/csve> .

Table 3: Hyper-parameters of CSVE evaluation

Hyper-parameters	Value and description
B	5, number of ensembles in dynamics model
α	10, to control the penalty of OOD states
τ	10, budget parameter in Eq. 8
β	In Gym domain, 3 for random and medium tasks, 0.1 for the other tasks; In Adroit domain, 30 for human and cloned tasks, 0.01 for expert tasks
γ	0.99, discount factor.
H	1 million for Mujoco while 0.1 million for Adroit tasks.
w	0.005, target network smoothing coefficient.
lr of actor	3e-4, policy learning rate
lr of critic	1e-4, critic learning rate

C Additional Ablation Study

Effect of model errors. Compared to traditional model-based offline RL algorithms, CSVE exhibits greater resilience to model biases. To access this resilience quantitatively, we measured the performance impact of model biases using the average L2 error in transition prediction as an indicator. As shown in Fig. 3, the influence of model bias on RL performance in CSVE is marginal. Specifically, in the halfcheetah task, there is no observable impact of model errors on scores, model errors show no discernible impact on scores. For the hopper and walker2d tasks, only a minor decline in scores is observed as the errors escalate.

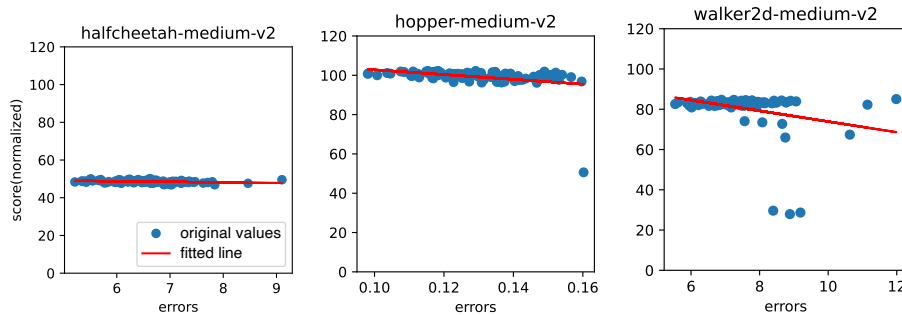


Figure 3: Effect of the model biases to performance scores. The correlation coefficient is -0.32 , -0.34 , and -0.29 respectively.

D Experimental Details and Complementary Results

D.1 Hyper-parameters of CSVE evaluation in experiments

Table 3 provides a detailed breakdown of the hyper-parameters used for evaluating CSVE in our experiments.

D.2 Details of Baseline CQL-AWR

To facilitate a direct comparison between the effects of conservative state value estimation and Q-value estimation, we formulated a baseline method named CQL-AWR as detailed below:

$$\hat{Q}^{k+1} \leftarrow \arg \min_Q \alpha (E_{s \sim D, a \sim \pi(a|s)}[Q(s, a)] - E_{s \sim D, a \sim \hat{\pi}_\beta(a|s)}[Q(s, a)]) + \frac{1}{2} E_{s, a, s' \sim D} [(Q(s, a) - \hat{\beta}_\pi \hat{Q}^k(s, a))^2]$$

$$\pi \leftarrow \arg \min_{\pi'} L_\pi(\pi') = -E_{s, a \sim D} \left[\log \pi'(a|s) \exp \left(\beta \hat{A}^{k+1}(s, a) \right) \right] - \lambda E_{s \sim D, a \sim \pi'(s)} \left[\hat{Q}^{k+1}(s, a) \right]$$

where $\hat{A}^{k+1}(s, a) = \hat{Q}^{k+1}(s, a) - \mathbb{E}_{a \sim \pi} [\hat{Q}^{k+1}(s, a)]$.

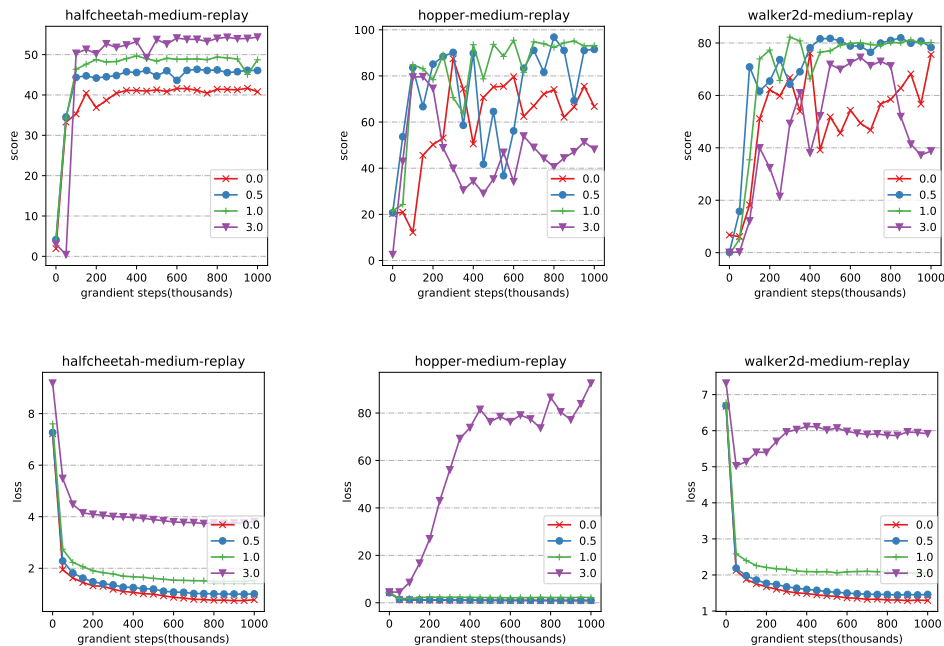


Figure 4: Effect of λ to Score (upper figures) and L_{π} loss in Eq. 9 (bottom figures)

In CQL-AWR, the critic adopts a standard CQL equation, while the policy improvement part uses an AWR extension combined with novel action exploration as denoted by the conservative Q function. When juxtaposed with our CSVE implementation, the policy segment of CQL-AWR mirrors ours, with the primary distinction being that its exploration is rooted in a Q-based and model-free approach.

D.3 Reproduction of COMBO

In Table 1 of our main paper, we used the results of COMBO as presented in the literature [23]. Here we detail additional attempts to reproduce the results and compare the performance of CSVE with COMBO.

Official Code. We initially aimed to rerun the experiment using the official COMBO code provided by the authors. The code is implemented in Tensorflow 1.x and relies on software versions from 2018. Despite our best efforts to recreate the computational environment, we encountered challenges in reproducing the reported results. For instance, Fig. 5 illustrates the asymptotic performance on medium datasets up to 1000 epochs, where the scores have been normalized based on SAC performance metrics. Notably, for both the hopper and walker2d tasks, the performance scores exhibited significant variability. The average scores over the last 10 epochs for halfcheetah, hopper, and walker2d were 71.7, 65.3, and -0.26, respectively. Furthermore, we observed that even when using the D4RL v0 dataset, COMBO demonstrated similar performance patterns when recommended hyper-parameters were applied.

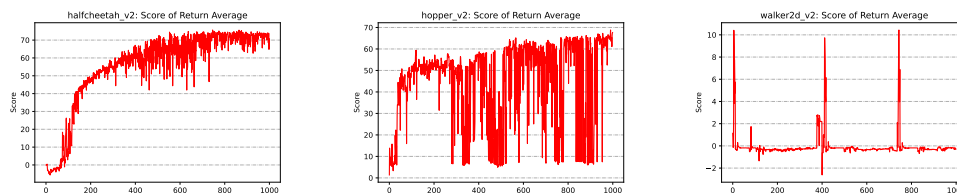


Figure 5: Return of official COMBO implementation on D4RL mujoco v2 tasks, fixing seed=0.

JAX-based optimized implementation Code [35]. We also tested one recent re-implementation available in RIQL. This version is regarded as the most highly-tuned implementation to date. The results of our tests can be found in Fig.6. For the random and expert datasets, we applied the same hyper-parameters as those used for the medium and medium-expert datasets, respectively. For all other datasets, we adhered to the default hyper-parameters provided by the authors [35]. Despite these efforts, when we compared our outcomes with the original authors' results (as shown in Table 10 and Fig.7 of [35]), our reproduced results consistently exhibited both lower performance scores and greater variability.

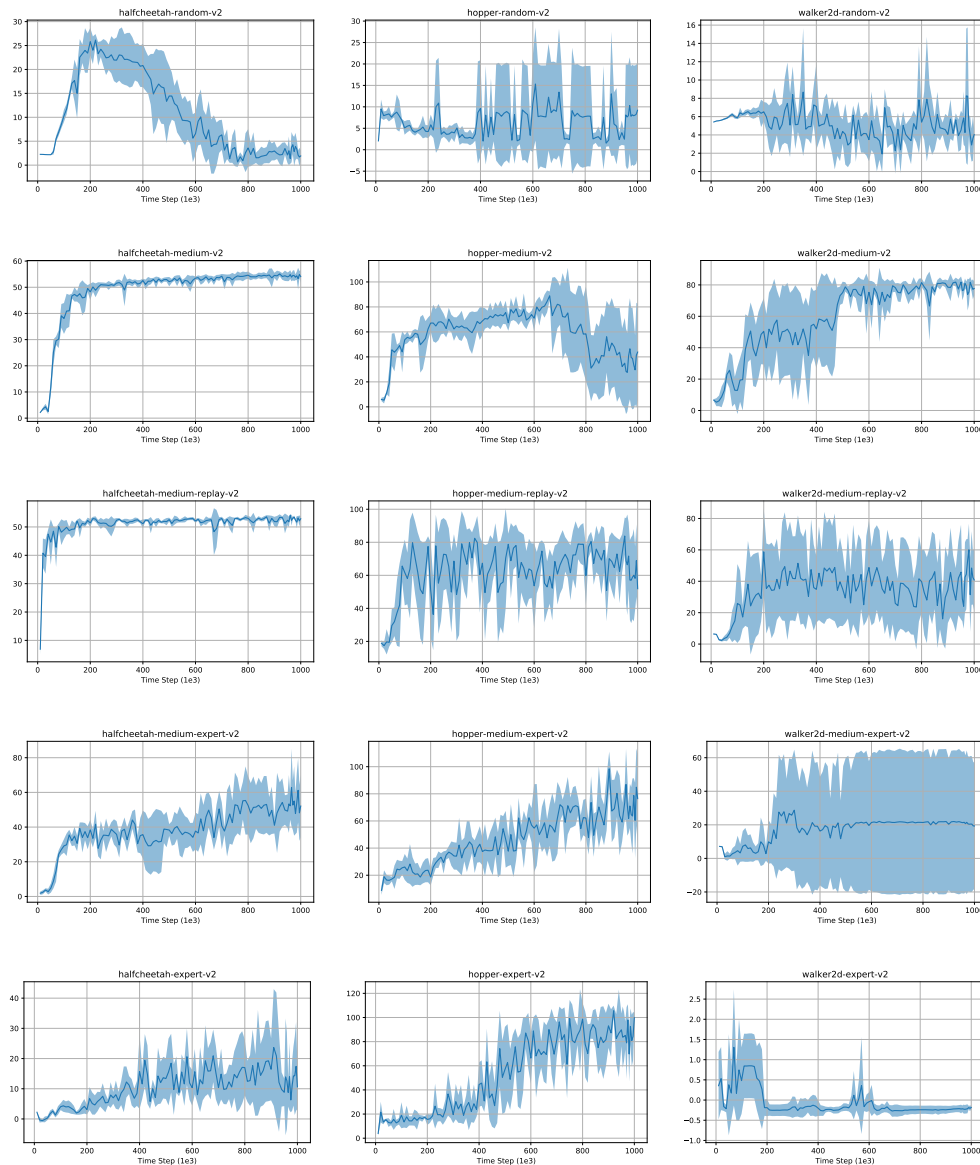


Figure 6: Return of an optimized COMBO implementation[35] on D4RL mujoco v2 tasks. The data are obtained by running with 5 seeds for each task, and the dynamics model has 7 ensembles.

D.4 Effect of Exploration on Near Dataset Distributions

As discussed in Section 3.1 and 4.2, the appropriate selection of exploration on the distribution (d) beyond data (d_u) should help policy improvement. The factor λ in Eq. 10 controls the trade-off on such 'bonus' exploration and complying with the data-implied behavior policy.

In section 5.2, we examined the effect of λ on the medium datasets of mujoco tasks. Now let us further take the medium-replay type of datasets for more analysis of its effect. In the experiments, with fixed $\beta = 0.1$, we investigate λ values of $\{0.0, 0.5, 1.0, 3.0\}$. As shown in the upper figures in Fig. 4, λ shows an obvious effect on policy performance and variances during training. In general, there is a value under which increasing λ leads to performance improvement, while above which further increasing λ hurts performance. For example, with $\lambda = 3.0$ in hopper-medium-replay task and walker2d-medium-replay task, the performance gets worse than with smaller λ values. The value of λ is task-specific, and we find that its effect is highly related to the loss in Eq. 9 which can be observed by comparing the bottom and upper figures in Fig. 4. Thus, in practice, we can choose proper λ according to the above loss without online interaction.

D.5 Conservative State Value Estimation by Perturbing Data State with Noise

In this section, we investigate a model-free method for sampling OOD states and compare its results with the model-based method adopted in section 4.

The model-free method samples OOD states by randomly adding Gaussian noise to the sampled states from the data. Specifically, we replace the Eq.5 with the following Eq. 34, and other parts are consistent with the previous technology.

$$\hat{V}^{k+1} \leftarrow \arg \min_V L_V^\pi(V; \widehat{Q}^k) = \alpha \left(E_{s \sim D, s' = s + N(0, \sigma^2)} [V(s')] - E_{s \sim D} [V(s)] \right) + E_{s \sim D} \left[\left(E_{a \sim \pi(\cdot|s)} [\widehat{Q}^k(s, a)] - V(s) \right)^2 \right]. \quad (34)$$

The experimental results on the Mujoco control tasks are summarized in Table 4. As shown, with different noise levels (σ^2), the model-free CSVE perform worse than our original model-based CSVE implementation; and for some problems, the model-free method shows very large variances across seeds. Intuitively, if the noise level covers the reasonable state distribution around data, its performance is good; otherwise, it misbehaves. Unfortunately, it is hard to find a noise level that is consistent for different tasks or even the same tasks with different seeds.

Table 4: Performance comparison on Gym control tasks. The results of different noise levels are over three seeds.

		CQL	CSVE	$\sigma^2=0.05$	$\sigma^2=0.1$	$\sigma^2=0.15$
Random	HalfCheetah	17.5 ± 1.5	26.7 ± 2.0	20.8 ± 0.4	20.4 ± 1.3	18.6 ± 1.1
	Hopper	7.9 ± 0.4	27.0 ± 8.5	4.5 ± 3.1	14.2 ± 15.3	6.7 ± 5.4
	Walker2D	5.1 ± 1.3	6.1 ± 0.8	3.9 ± 3.8	7.5 ± 6.9	1.7 ± 3.5
Medium	HalfCheetah	47.0 ± 0.5	48.6 ± 0.0	48.2 ± 0.2	47.5 ± 0.0	46.0 ± 0.9
	Hopper	53.0 ± 28.5	99.4 ± 5.3	36.9 ± 32.6	46.1 ± 2.1	18.4 ± 30.6
	Walker2D	73.3 ± 17.7	82.5 ± 1.5	81.5 ± 1.0	75.5 ± 1.9	78.6 ± 2.9
Medium Replay	HalfCheetah	45.5 ± 0.7	54.8 ± 0.8	44.8 ± 0.4	44.1 ± 0.5	43.8 ± 0.4
	Hopper	88.7 ± 12.9	91.7 ± 0.3	85.5 ± 3.0	78.3 ± 4.3	70.2 ± 12.0
	Walker2D	81.8 ± 2.7	78.5 ± 1.8	78.7 ± 3.3	76.8 ± 1.3	66.8 ± 4.0
Medium Expert	HalfCheetah	75.6 ± 25.7	93.1 ± 0.3	87.5 ± 6.0	89.7 ± 6.6	93.8 ± 1.6
	Hopper	105.6 ± 12.9	95.2 ± 3.8	63.2 ± 54.4	99.0 ± 11.0	37.6 ± 63.9
	Walker2D	107.9 ± 1.6	109.0 ± 0.1	108.4 ± 1.9	109.5 ± 1.3	110.4 ± 0.6
Expert	HalfCheetah	96.3 ± 1.3	93.8 ± 0.1	59.0 ± 28.6	67.5 ± 21.9	75.3 ± 27.3
	Hopper	96.5 ± 28.0	111.2 ± 0.6	67.3 ± 57.7	109.2 ± 2.4	109.4 ± 2.1
	Walker2D	108.5 ± 0.5	108.5 ± 0.0	109.7 ± 1.1	108.9 ± 1.6	108.6 ± 0.3